

# Dual-Space Feedforward Control of a Redundantly Actuated Parallel Manipulator for Very High Speed Applications

G. Sartori-Natal\* A. Chemori\* M. Michelin\* F. Pierrot\*

\* *Laboratoire d'Informatique, de Robotique et de Microélectronique de Montpellier (LIRMM), Univ. Montpellier 2 - CNRS, 161 rue Ada, 34095 Montpellier Cedex 5, France (e-mail: sartorinat@lirmm.fr).*

---

**Abstract:** This paper deals with dual-space control of R4 redundantly actuated parallel manipulator for very high acceleration applications. This controller consists in a PID in the Cartesian space complied with a feedforward of the desired acceleration in both Cartesian and articular spaces for tracking performance improvements: models show that this “dual-space” control strategy is an efficient way to implement computed torque control. For comparison purposes, experiments were made with a Cartesian PID until 20G. Experimental results show that the proposed control scheme is considerably better than the PID in the Cartesian space, and that a good tracking performance could be achieved even for the very high acceleration of 40G (equivalent to more than 425 pick-and-place cycles per minute).

*Keywords:* Parallel manipulators, PID control, Feedforward control, Trajectory tracking, Pick-and-place.

---

## 1. INTRODUCTION

In order to perform very high speed/acceleration tasks, it is well known that parallel manipulators have important advantages in comparison to serial manipulators. One of its main disadvantages, however, is the abundance in singularities in the workspace (Kock et al. (1998)). If singularities cannot always be eliminated by actuation redundancy, their locii can be modified (Gosselin et al. (1990), Park et al. (1999)). Actuation redundancy might also be a way to reach higher accelerations or to improve the homogeneity of acceleration performance over the workspace (this was the basic conjecture in Corbel et al. (2010)), and can also allow for more safety in case of breakdown of individual actuators (Yi et al. (2006), Roberts et al. (2008)).

Considering these features, the R4 parallel manipulator Corbel et al. (2010) (which can be seen as a redundant Delta robot (Clavel (1988))), has three degrees-of-freedom (*dof*) and four actuators. It was designed to have the capability of reaching 100G of acceleration. The number of actuators was chosen such that a good compromise between the gain in acceleration capabilities and the overall cost of the robot could be obtained.

In the literature, several control schemes of parallel manipulators in joint space and in Cartesian space have been proposed. In the joint space, Proportional-Derivative (PD) controllers were implemented in Ghorbel et al. (2000), Wu et al. (2002), PID controllers tuned with elaborated methods (adapted for Parallel Kinematic Machines: PKMs)

were proposed in Zhiyong et al. (2004), Yang et al. (2006), nonlinear PD control was proposed in Ouyang et al. (2002), Su et al. (2004) and artificial-intelligence based control in Begon et al. (1995), Chung et al. (1999). The nonlinear dynamics is not considered in these (kinematic) controllers, so the complex computation of dynamics can be avoided and the controller design can be simplified considerably. However, these controllers do not always produce high performance, and there is no guarantee of stability at the high speed (Shang et al. (2010)). Unlike the kinematic control strategies, full dynamic model of parallel manipulator is taken into account in the dynamic control strategies. So, the nonlinear dynamics of the manipulator can be compensated and higher performance can be achieved with dynamic strategies. Traditional dynamic strategies such as the augmented PD (APD) and the computed-torque controllers were implemented in Cheng et al. (2003), Paccot et al. (2009). Model-based adaptive controllers have been proposed in Honegger et al. (1997), Honegger et al. (2000), Craig (1988), Sartori-Natal et al. (2009). All mentioned controllers were designed in the joint space. Nevertheless, we are usually concerned about the trajectory tracking in the task space. Especially for the parallel manipulators with redundant actuators, where the effect of the redundant actuators to the end-effector motion can be fully considered (Shang et al. (2010)). In the task space, the PID, the augmented PD (APD) and the computed torque controller have been compared in Paccot et al. (2009). In Shang et al. (2009), a nonlinear computed torque controller was designed in order to overcome the problem that its PD algorithm is not robust against modeling errors and nonlinear frictions. For the case of parallel manipulators with redundant actuation, adaptive

---

\* This work is supported by ECHORD PRADA: an European project.

controllers were designed in the task space to take into account the effect of redundant actuation in Wang et al. (2009), Shang et al. (2010).

The main objective of the present work is to reach very high accelerations with a simple control approach that would have a small computation time and would be able to maintain a good tracking performance. This controller consists in using a PID in the Cartesian space to cope with actuation redundancy issues, with the addition of the Cartesian and articular accelerations feedforward terms (which will be shown to directly compensate for the dynamics of the system, in a similar way to a “computed torque” controller), obtaining an important improvement of the tracking performance with comparison to the Cartesian PID controller alone.

This paper is organized as follows. In section 2, a brief description of the R4 parallel manipulator is presented. The proposed control approach is detailed in section 3. Section 4 is devoted to the pick-and-place trajectory generation. The experimental results are presented in section 5. A discussion about the conclusions and future works is made in section 6.

## 2. R4 PARALLEL MANIPULATOR

### 2.1 Description of the R4 robot

The R4 parallel manipulator (cf. Fig. 1) has the following main characteristics:

- (1) 3-*dof* (translations along X-Y-Z axis) and 4 actuators (redundantly actuated),
- (2) Each motor has a maximum torque of 127N.m,
- (3) A workspace of at least a cylinder of 300 mm radius and 100 mm height.

Its CAD schematic view and its side view are shown in Fig. 1. Its geometrical and dynamic parameters are summarized in table 1 and illustrated in Fig. 2, being  $r_b$  the horizontal distance between  $O_b$  and  $B_i$ , and  $r_{tp}$  the horizontal distance between  $O_b$  and  $P_i$ .

### 2.2 Simplified Direct Dynamics

Some simplifications on the dynamics of the robot were made during its design phase, in order to evaluate which configuration would be the most optimal in terms of performance and cost, such as the neglect of the joint frictions (as the components of the robot were designed in order to have very small frictions between them), the inertia of the forearms, and the gravity acceleration (since the case studies considered very high accelerations). These assumptions are further discussed in Pierrot et al. (2009).

Table 1. Geometric/Dynamic Parameters

$r_b$ [m]	$r_{tp}$ [m]	$l_i$ [m]	$L_i$ [m]
0.135	0.05	0.2	0.53
$M_{tp}$ [kg]	$M_{forearm}$ [kg]	$I_{act}$ [kg.m <sup>2</sup> ]	$I_{arm}$ [kg.m <sup>2</sup> ]
0.2	0.065	0.003	0.005

The expression of R4's simplified direct dynamic model is given by Corbel et al. (2010):

$$\ddot{x} = (M_T + J_m^T I_T J_m)^{-1} J_m (\Gamma - I_T \dot{J}_m \dot{x}) \quad (1)$$

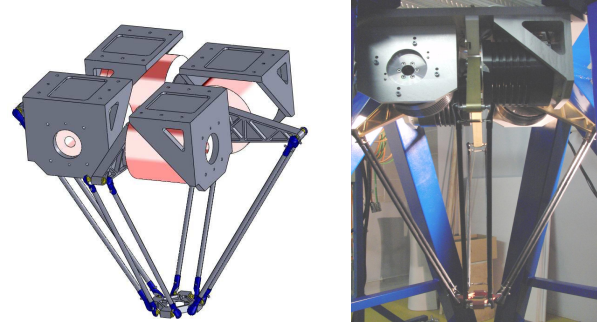


Fig. 1. The R4 parallel manipulator: Schematic view of the CAD design (left), side view of the robot prototype (right)

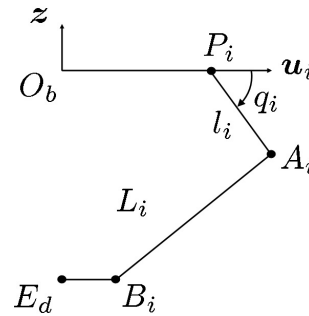


Fig. 2. The R4 parallel manipulator geometric parameters

where  $\dot{x} \in \mathcal{R}^m$  and  $\ddot{x} \in \mathcal{R}^m$  are the vectors of Cartesian velocities and accelerations;  $M_T = \text{Diag}\{M_{tp} + n \frac{M_{forearm}}{2}\}_{m \times m} = M_{tot} I_{m \times m}$  is a diagonal matrix with  $m$  diagonal terms, being  $M_{tp}$  the mass of the traveling plate,  $M_{forearm}$  the mass of the forearm,  $M_{tot}$  the scalar value of the diagonal of  $M_T$ ,  $m$  the number of degrees-of-freedom ( $m = 3$ ) and  $n$  the number of motors ( $n = 4$ );  $I_T = \text{Diag}\{I_{act} + I_{arm}\}_{n \times n} = I_{tot} I_{n \times n}$  is a diagonal matrix with  $n$  diagonal terms, where  $I_{act}$  and  $I_{arm}$  are the inertia of the actuators and the inertia of the arms, respectively, and  $I_{tot}$  is the scalar value of the diagonal of  $I_T$ ;  $J_m \in \mathcal{R}^{n \times m}$  and  $\dot{J}_m \in \mathcal{R}^{n \times m}$  are the generalized inverse Jacobian matrix and its first derivative, respectively; and  $\Gamma \in \mathcal{R}^n$  represents the torques generated by the actuators. For further details on the mechanical design of the R4 parallel manipulator, the reader is referred to Corbel et al. (2010).

## 3. PROPOSED CONTROL SCHEME: A DUAL-SPACE FEEDFORWARD CONTROLLER

As mentioned in section 1, the R4 parallel manipulator is redundantly actuated (4 motors and 3 *dof*). This characteristic has important advantages in terms of mechanical capabilities of the robot, but in terms of control, new issues arise: not only classical articular control schemes are unable to deal with dynamic effects on the Cartesian space, but they are also unable to cope with the actuation redundancy (the integral term will be disturbed by kinematic inconsistencies). In order to deal with this issue, a Cartesian PID was firstly proposed. Its scheme is presented in Fig. 3.

The dual-space feedforward controller consists basically in a PID in the Cartesian space and a feedforward of

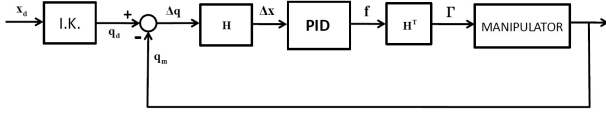


Fig. 3. Block diagram of the proposed Cartesian PID controller

both desired Cartesian/articular accelerations to take the dynamics of the system in consideration and improve the tracking performance. This control approach is illustrated in Fig. 4.

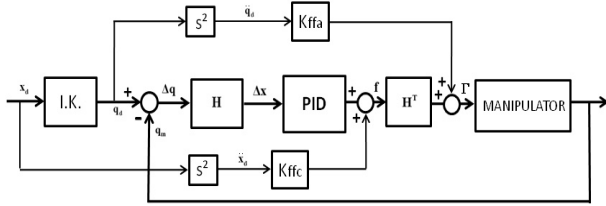


Fig. 4. Block diagram of the proposed dual-space controller

The desired trajectory is given in the Cartesian space ( $x_d$ ). As only the joint positions are measured ( $q_m$ ), this desired trajectory is converted to the joint space ( $q_d$ ) through the inverse kinematics (block I.K.) of the robot (Corbel et al. (2010)), such that the corresponding tracking error can be obtained. The joint tracking errors ( $\Delta q$ ) must then be reconverted to the Cartesian space in order to be used by the PID controller. As the joint tracking errors are assumed to be significantly small, and the sampling time ( $\Delta t$ ) is of only  $0.1ms$  ( $10^{-4}s$ ), let  $\frac{\Delta q}{\Delta t} \simeq \frac{dq}{dt}$ . Then, it is recalled that  $\dot{q} = J_m \dot{x}$ . This relation has an unique solution, but in the case of redundantly actuated systems ( $n > m$ ), the inverse relation will have infinite solutions. In order to cope with this issue, the pseudo-inverse of  $J_m$  is used instead (the pseudo-inverse has the property of generating a solution with the minimum Euclidian norm). Therefore, one has:

$$\dot{x} = J_m^+ \dot{q} = H \dot{q} \quad (2)$$

where  $H$  is the pseudo-inverse of  $J_m$ , that is  $H = J_m^+ = (J_m^T J_m)^{-1} J_m^T$ . From (2), one can conclude that the relation between the joint errors and the Cartesian errors ( $\Delta x$ ) can be considered as  $\Delta x \simeq H \Delta q$ .

The resulting forces ( $f$ ) to be applied on the end-effector will be the sum of the Cartesian PID with the feedforward of the desired Cartesian accelerations (which were obtained by deriving the desired Cartesian trajectories twice). Now, the resulting forces need to be converted to the joint space, as the control inputs that will be sent to the robot are the torques ( $\Gamma$ ) to be applied by the motors. For this purpose, it is known that from (2), the following relation can be obtained:

$$\Gamma = H^T f \quad (3)$$

The desired joint trajectories are also derived twice in order to obtain the desired accelerations for its feedforward term. The following control law is then proposed:

$$\Gamma = H^T f + K_{ffa} \ddot{q}_d \quad (4)$$

being  $f = K_p e(t) + K_i \int e(t) dt + K_d \frac{de(t)}{dt} + K_{ffc} \ddot{x}_d$  the force applied on the traveling plate,  $e = \Delta x$ ,  $K_p$ ,  $K_i$  and  $K_d$  are the Cartesian PID gains,  $K_{ffc}$  the Cartesian acceleration feedforward gain and  $K_{ffa}$  is the joint acceleration feedforward gain. The PID in the Cartesian space was tuned experimentally through the procedure of small steps, as this is a very nonlinear system and theoretical design methods are more suitable for linear systems. The feedforward gains were calculated analytically from the dynamic model of the R4 parallel manipulator as follows.

### 3.1 Calculation of the feedforward gains

In order to calculate the feedforward gains of the dual-space controller, it is necessary to take into consideration the dynamics of the system, which is represented by (1). By multiplying both sides by  $(M_T + J_m^T I_T J_m)$ , one has:

$$(M_{tot} + J_m^T I_T J_m) \ddot{x} = J_m^T (\Gamma - I_T \dot{J}_m \dot{x}) \quad (5)$$

By separating the torques ( $\Gamma$ ) on the left side and multiplying both sides by the pseudo-inverse of  $J_m^T$  (which will be named  $H^T$ ), the following expression is obtained:

$$\Gamma = H^T M_T \ddot{x} + I_T (J_m \ddot{x} + \dot{J}_m \dot{x}) \quad (6)$$

If one takes into consideration that  $(J_m \ddot{x} + \dot{J}_m \dot{x})$  is equal to the articular acceleration vector ( $\ddot{q}$ ), the final expression arises:

$$\Gamma = H^T M_T \ddot{x} + I_T \ddot{q} \quad (7)$$

By direct analysis of Fig. 4, the value of the gains that should multiply  $\ddot{x}_d$  and  $\ddot{q}_d$  are, respectively,  $K_{ffc} = M_{tot} = 0.33$  and  $K_{ffa} = I_{tot} = 0.012$ . The gains of the proposed control scheme are shown in table 2.

Table 2. Parameters of the Proposed Controller

$K_p$	$K_i$	$K_d$	$K_{ffc}$	$K_{ffa}$
8000	600	40	0.33	0.012

## 4. TRAJECTORY GENERATION

In this section, two case studies will be presented and detailed. The first one consists in a spiral movement (cf. Fig. 5) that was implemented for a maximum acceleration of 20G (which provided a frequency of 6.5 revolutions per second) on the Cartesian PID and on the proposed dual-space Cartesian/articular controller. The second one consists in a double pick-and-place trajectory (cf. Fig. 6) that was implemented for a maximum acceleration of 40G only with the dual-space controller (for safety reasons).

### 4.1 First case study: Spiral movements in X-Y plane

The desired X-Y trajectory is described as follows:

$$\begin{cases} x_d = K_{mod} 0.125 \sin(13\pi t) \\ y_d = K_{mod} 0.125 \sin(13\pi t + \frac{\pi}{2}) \end{cases} \quad (8)$$

being  $K_{mod} = 0.5 \sin(\frac{2\pi t}{15} + \frac{3\pi}{2} - \frac{2\pi}{5})$  a modulation function that guarantees a smooth variation of the circle's radius in order to avoid an abrupt start/finish of experiments. The obtained curve is illustrated in Fig. 5. In this experiment, the robot goes to its initial position  $((0, 0, -0.55)m)$

and stops, and then the radius of the circular movement increases smoothly until it reaches  $0.125m$  and then decreases smoothly until the robot stops.

The objective of this case study is to evaluate the trajectory tracking performance that would be obtained by the addition of the joint acceleration feedforward to the Cartesian PID controller. As will be detailed in section 5, this performance improvement allowed for a safer increase of the acceleration/velocity of the robot until  $40G$ , which was achieved on the second case study.

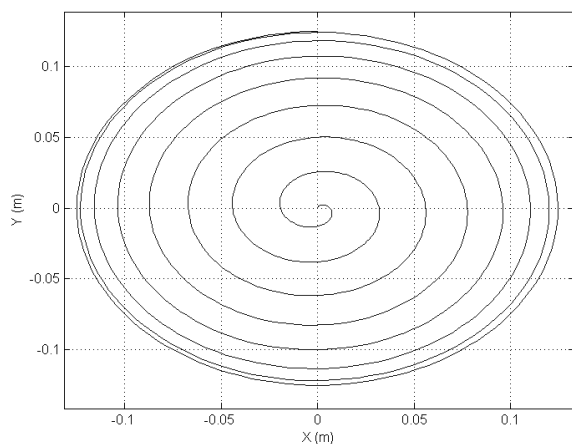


Fig. 5. Top view of the trajectory used in the first case study (spiral in the X-Y plane)

#### 4.2 Second case study: 3D pick-and-place movements

The objective of this case study is to evaluate the capability of the proposed control approach to deal with very high accelerations/velocities in a pick-and-place task. The desired trajectory was chosen such that movements of different distances would have to be performed in the same amount of time, which would require different accelerations/velocities for each one of them, demonstrating the good applicability of the proposed control scheme. The sequence of movements that was executed in this case study is the following:

- (1) **Pick 1 - Place 1:** From  $(-0.1,0.1)m$  to  $(0.1,-0.1)m$ ,
- (2) **Place 1 - Pick 2:** From  $(0.1,-0.1)m$  to  $(0.1,0.1)m$ ,
- (3) **Pick 2 - Place 2:** From  $(0.1,0.1)m$  to  $(-0.1,-0.1)m$ ,
- (4) **Place 2 - Pick 1:** From  $(-0.1,-0.1)m$  to  $(-0.1,0.1)m$ .

Each movement was performed in  $0.07s$  ( $0.28s$  for the whole cycle) and their maximum height was equal to  $5cm$ .

The corresponding reference trajectory is generated by an algorithm based on a polynomial interpolation of degree five presented in Khalil et al. (2004). This algorithm guarantees the continuity of the movement in position, velocity and also in acceleration. Its main idea consists in reaching a desired final position from a given initial position in a certain time duration (which is chosen by the user).

## 5. REAL-TIME EXPERIMENTAL RESULTS

The objective of this section is to present and discuss the real-time experimental results obtained by the application

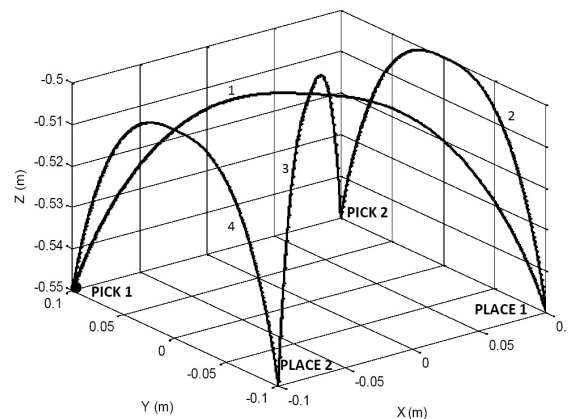


Fig. 6. Isometric view of the trajectory used in the second case study (3D pick-and-place)

of the proposed control schemes described in section 3 on the parallel manipulator R4 described in section 2, in order to track the reference trajectories detailed in section 4.

The proposed control schemes were implemented in Simulink/Matlab, being compiled and uploaded to a XPC/Target computer, which managed the real-time task with a sampling frequency of  $10KHz$ , which corresponds to a sampling time of  $0.1ms$ .

#### 5.1 First case study: Spiral movements in X-Y plane

The obtained results for this scenario are given by Figs. 7-8. The robot goes from an arbitrary position to the desired initial position  $(0,0,-0.55)m$  and then the radius of the circle starts to increase until it reaches  $0.125m$  (reaching a maximum acceleration of  $20G$ ), then it decreases in the same way until the robot stops. In order to compare the performance of both controllers, Figs. 7-8 show a zoom at the time interval of maximum amplitude.

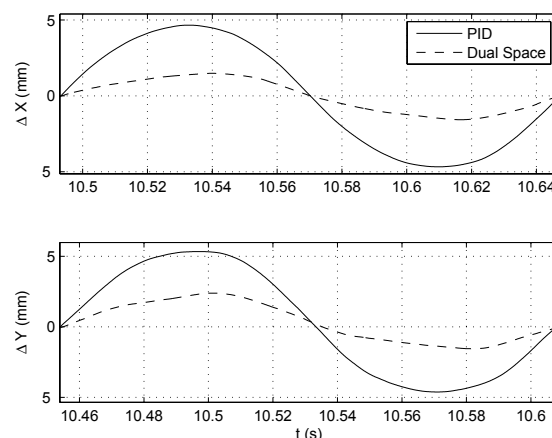


Fig. 7. Tracking errors for the PID controller (solid) and for the dual-space controller (dashed)

By analyzing Fig. 7, it is possible to notice that the dual-space controller provided a considerably better tracking performance than the classical Cartesian PID. While the former kept the tracking error between  $[-4.62, 5.33]mm$

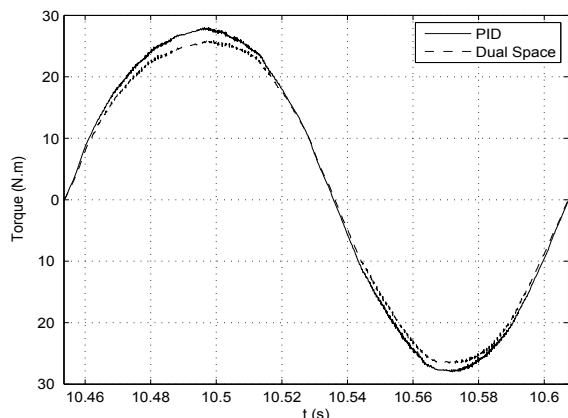


Fig. 8. Torques for the PID controller (solid) and for the dual-space controller (dashed)

(4% of peak-to-peak error), the latter kept it between  $[-1.55, 2.34]mm$  (1.56%) (cf. Fig. 7), which means a peak-to-peak improvement of approximately 60%. The Root Mean Square Error (RMSE) shows an equivalent improvement in performance (1.3mm against 3.6mm, which means an improvement of approximately 64%). Another advantage of the dual-space controller was that its control signal had an approximately 6% smaller peak-to-peak ( $[-26.4, 26.2]Nm$  against  $[-28, 28]Nm$ ) than the Cartesian PID (cf. Fig. 8). These results are summarized in table 3. With the conclusion that the dual-space controller can provide a considerably better tracking performance than the Cartesian PID, the latter was discarded for the next case study.

Table 3. Performance comparison between the proposed control approach and the Cartesian PID controller

Performance	PID	Dual-space
Error peaks	$[-4.62, 5.33]mm$	$[-1.55, 2.34]mm$
RMSE	3.6mm	1.3mm
Control signals	6% smaller peak-to-peak value	

### 5.2 Second case study: 3D pick-and-place movements

In the following experiment, the robot goes from an arbitrary position to the initial position  $(-0.1, 0.1, -0.55)m$  and then two cycles of the proposed pick-and-place trajectory start. The obtained results for this scenario are depicted in Figs. 9-10.

By analyzing Fig. 9, it is possible to notice that the proposed control scheme was able to maintain a good tracking performance even for such fast movements. Fig. 10 shows that the dual-space controller kept the tracking errors of the X-Y axis between  $[-3.21, 4.4]mm$  (3.8% of peak-to-peak error) and the tracking errors of the Z-axis between  $[-6.66, 6.27]mm$  (25.9% of peak-to-peak error). Even though the errors in the Z-axis may seem relatively big, it is important to emphasize that its peak errors happen during the displacement of the platform, while it is known that the control objective of a pick-and-place task is to obtain the best precision around the stop points (which take place on the periodical bottom of the Z-axis reference trajectory, being the circled neighbourhood of  $t = 4.25s$

an example). In Figs. 9 and 10 it is clear that around the stop points the errors are satisfactorily small (smaller than 1.5mm). None of the motors has reached even half of its limit of 127Nm. These results are summarized in table 4.

It is also interesting to mention that the proposed control architecture was simulated using the dynamic model of the robot to demonstrate its tracking performance and compare the obtained results with those obtained with the real system. This simulation was conducted in the same conditions as in the experiments, and the tracking errors (cf. Figs. 9-10) were not far from the ones obtained in the executed experiments, especially for the X - Y axes.

Table 4. Tracking performance obtained with the proposed controller for the 40G pick-and-place trajectory

Performance	Dual-space
Error peaks (X-Y)	$[-3.21, 4.4]mm$ (3.8%)
Error peaks (Z) / displacement	$[-6.66, 6.27]mm$ (25.9%)
Error peaks (Z) / stop points	$[-1.5, 1.5]mm$ (6%)
Control Signals	Smooth/far from motor limits

The obtained acceleration was slightly higher than 40G ( $\frac{400.3}{9.81}m/s^2 \rightarrow 40.8G$ ). This measurement was made with an external accelerometer (Silicon Designs 2460-200, which senses accelerations in all 3 axis and has a measurement limit of  $\pm 200G$ ) attached to the end-effector.

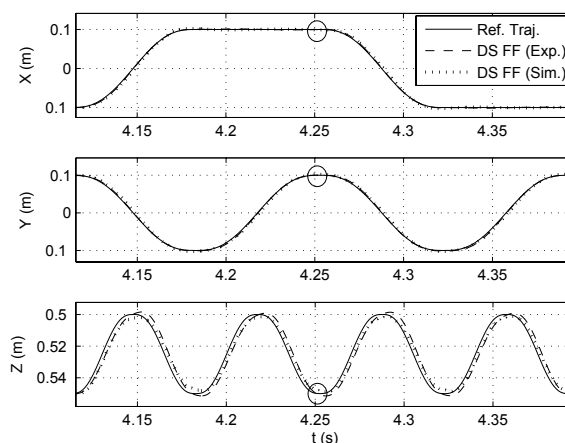


Fig. 9. Trajectory tracking for 40G of acceleration

## 6. CONCLUSION AND FUTURE WORKS

This paper dealt with the control of the redundantly actuated parallel manipulator R4 for very fast pick-and-place applications. The proposed control scheme consisted in a PID in the Cartesian space complied with a feedforward of the desired acceleration in both Cartesian and articular spaces, firstly for a spiral movement in X and Y-axis (maximum acceleration of 20G) and then for a pick-and-place task (maximum acceleration of 40G). By analyzing the results of the first case study, it was possible to notice that the proposed controller had a considerably better performance than only the Cartesian PID controller, being the latter discarded for the second case study for safety reasons. It was then possible to notice that the proposed dual-space Cartesian/articular controller was able to provide

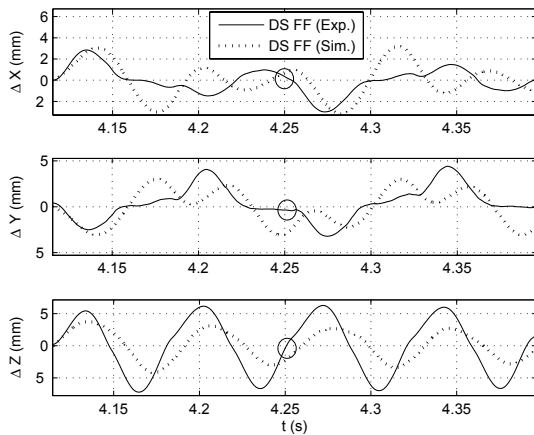


Fig. 10. Tracking errors for 40G of acceleration

a good tracking performance even in such fast pick-and-place tasks (equivalent to more than 425 pick-and-place cycles per minute). In the future, other control approaches to be investigated/proposed will be evaluated for higher accelerations and/or for different load conditions.

#### REFERENCES

- Begon, P., Pierrot, F., and Dauchez, P. (1995). Robot control and parameter estimation with only joint position measurements. *Proc. IEEE Int. Conf. Robot. Autom.*, 1178–1183.
- Cheng, H., Yiu, Y.K., and Li, Z. X. (2003). Dynamics and control of redundantly actuated parallel manipulators. *IEEE Trans. Mechatronics*, volume 8, 483–491.
- Chung, I. F., Chang, H. H., and Lin C. T. (1999). Fuzzy control of a six-degree motion platform with stability analysis. *Proc. IEEE Int. Conf. Syst. Man. Cybern.*, 325–330.
- Clavel, R. (1988). Delta, a fast robot with parallel geometry. *International Symposium on Industrial Robots*, 91–100.
- Corbel, D., Gouttefarde, M., Company, O., and Pierrot, F. (2010). Towards 100g with pkm. Is actuation redundancy a good solution for pick-and-place? *Proc. IEEE Int. Conf. Robot. Autom.*, 4675–4682.
- Craig, J. J. (1988). *Adaptive Control of Mechanical Manipulators*, Addison-Wesley Publishing Company, 1178–1183.
- Ghorbel, F. H., Chatelat, O., Gunawardana, R., and Longchamp, R. (2000). Modeling and set point control of closed-chain mechanisms: theory and experiment. *IEEE Trans. Control Syst. Technol.*, 801–815.
- Gosselin, C. and Angeles, J. (1990). Singularity analysis of closed-loop kinematic chains. *IEEE Trans. on Robotics Automat.*, volume 6, number 3, 281–290.
- Honegger, M., Codourey, A., and Burdet, E. (1997). Adaptive control of the hexaglide, a 6 dof parallel manipulator. *Proc. IEEE Int. Conf. Robot. Autom.*, 543–548.
- Honegger, M., Brega, R., and Schweitzer, G. (2000). Application of a nonlinear adaptive controller to a 6 dof parallel manipulator. *Proc. IEEE Int. Conf. Robot. Autom.*, 1930–1935.
- Khalil, W. and Dombre, E. (2004). *Modeling, identification & control of robots*, Butterworth-Heinemann.
- Kock, S. and Schumacher, W. (1998). A parallel x-y manipulator with actuation redundancy for high-speed and active-stiffness applications. *Proc. IEEE Int. Conf. Robot. Autom.*, 2295–2300.
- Ouyang, P. R., Zhang, W. J., and Wu, F. X. (2002). Nonlinear pd control for trajectory tracking with consideration of the design for control methodology. *Proc. IEEE Int. Conf. Robot. Autom.*, 4126–4131.
- Paccot, F., Andreff, N., and Martinet, P. (2009). A review on the dynamic control of parallel kinematic machines: theory and experiments. *Int. J. Rob. Research*, volume 28, number 3, 395–416.
- Park, F. C. and Kim, J. W. (1999). Singularity analysis of closed kinematic chains. *ASME Trans. J. Mech. Des.*, 32–38.
- Pierrot, F., Baradat, C., Nabat, V., Company, O., Krut, S., and Gouttefarde, M. (2009). Above 40g acceleration for pick-and-place with a new 2-dof pkm. *Proc. IEEE Int. Conf. Robot. Autom.*, 1794–1800.
- Roberts, R. G., Yu, H. G., and Maciejewski, A. A. (2008). Fundamental limitations on designing optimally fault-tolerant redundant manipulator. *IEEE Trans. Robotics*, volume 24, number 5, 1224–1237.
- Sartori-Natal, G., Chemori, A., Pierrot, F., and Company, O. (2009). Nonlinear dual mode adaptive control of par2: a 2-dof planar parallel manipulator, with real-time experiments. *Proc. IEEE Int. Conf. Intel. Robots and Systems*, 2114–2119.
- Shang, W. W. and Cong, S. (2009). Nonlinear computed torque control for a high-speed planar parallel manipulator. *Mechatronics*, volume 19, number 6, 987–992.
- Shang, W. W. and Cong, S. (2010). Nonlinear adaptive task space control for a 2-dof redundantly actuated parallel manipulator. *Nonlinear Dynamics*, volume 59, number 1, 61–72.
- Su, Y. X., Duan, B. Y., Zheng, C. H., Zhang, Y. F., Chen, G. D., and Mi, J. W. (2004). Disturbance-rejection high-precision motion control of a stewart platform. *IEEE Trans. Control Syst. Technol.*, volume 12, number 3, 364–374.
- Yang, Z.-Y., Huang, T. (2006). Parameter identification and tuning of the servo system of a 3-hss parallel kinematic machine. *Int. Journal of Adv. Manuf. Tech.*, volume 31, number 5, 621–628.
- Yi, Y., Mcinroy, J. E., and Chen, Y. X. (2006). Fault tolerance of parallel manipulators using task space and kinematic redundancy. *IEEE Trans. Robotics*, volume 22, number 5, 1017–1021.
- Wang, L., Lu, Z. T., Liu, X. P., Liu, K. F., and Zhang, D. (2009). Adaptive control of a parallel robot via backstepping technique. *Int. J. Systems, Contr. and Comm.*, volume 1, number 3, 312–324.
- Wu, F. X., Zhang, W. J., Li, Q., and Ouyang, P. R. (2002). Integrated design and pd control of high-speed closed-loop mechanisms. *J. Dyn. Syst. Meas. Control*, volume 124, number 4, 522–528.
- Zhiyong, Y. and Huang, T. (2004). Robot control and parameter estimation with only joint position measurements. *Proc. IEEE Int. Conf. Robot. Autom.*, 2249–2254.